

Shear viscosity at the Ising-nematic quantum critical point in two dimensional metals

Andreas Eberlein,¹ Aavishkar A. Patel,¹ and Subir Sachdev^{1,2}

¹*Department of Physics, Harvard University, Cambridge, Massachusetts 02138, USA*

²*Perimeter Institute for Theoretical Physics, Waterloo, Ontario, Canada N2L 2Y5*

(Dated: September 3, 2018)

In an isotropic strongly interacting quantum liquid without quasiparticles, general scaling arguments imply that the dimensionless ratio $(k_B/\hbar)\eta/s$, where η is the shear viscosity and s is the entropy density, is a universal number. We compute the shear viscosity of the Ising-nematic critical point of metals in spatial dimension $d = 2$ by an expansion below $d = 5/2$. The anisotropy associated with directions parallel and normal to the Fermi surface leads to a violation of the scaling expectations: η scales in the same manner as a chiral conductivity, and the ratio η/s diverges at low temperature (T) as $T^{-2/z}$, where z is the dynamic critical exponent for fermionic excitations dispersing normal to the Fermi surface.

I. INTRODUCTION

Recent experiments on graphene^{1,2} and PdCoO₂³ have displayed remarkable evidence for nearly-momentum-conserving hydrodynamic flow of the electron liquid. In clean Fermi liquids, hydrodynamic flow requires very clean samples with weak umklapp scattering so that electron-electron collisions lead to thermalization before there is significant momentum lost to the crystal³⁻⁶. However, rapid thermalization and hydrodynamics are natural properties of quantum critical systems⁷ and strange metals⁸⁻¹¹, and their consequences should be visible even in moderately clean samples. Graphene was proposed as a strange metal in which ill-defined quasiparticles lead to hydrodynamic flow at intermediate temperatures¹²⁻²³: the experiments also display evidence^{1,2,20-22} for the viscous drag of such flow. There have also been studies of viscous flow in high energy physics²⁴⁻²⁷ and ultracold atoms²⁸⁻³².

These experimental advances indicate that the time is ripe for exploring hydrodynamic electron flow in the ubiquitous strange metal regimes of the cuprates or the pnictides. These are metals without quasiparticle excitations, and so should exhibit hydrodynamic flow when impurities are dilute. We note the indirect evidence for such behavior in the photoemission experiments of Rameau *et al.*³³. To this end, here we examine the simplest model which realizes a metallic state without quasiparticles in two spatial dimensions, and compute its shear viscosity, η . We will study the quantum critical point (QCP) for the onset of Ising nematic order³⁴⁻³⁶ using its continuum field theoretic formulation using patches on the Fermi surface^{37,38}.

General scaling arguments (reviewed below) for a spatially isotropic system imply that η should scale in the same manner as the entropy density, s ; so

$$\eta/s \sim \hbar/k_B, \quad (1)$$

where the r.h.s. restores dimensions, and the prefactor is expected to be of order unity. (In $d = 2$ hydrodynamic long time tails can lead to logarithmic corrections to η ³⁹

which we ignore here, as we find much larger corrections). This is also the expectation from holographic studies of critical quantum liquids^{24,25,40-44}. A relationship of the form (1) appeared in string-theoretic realizations of strongly-coupled field theories²⁵, and has been widely used as a diagnostic of strongly-coupled non-quasiparticle dynamics in the quark-gluon plasma²⁴⁻²⁷.

Our main result is that Eq. (1) does not apply to many of the models of electronic strange metals without quasiparticles. Even without long-lived quasiparticles, such models have a Fermi surface at $T = 0$, which defines momenta with singular low energy excitations; more precisely, the Fermi surface is the locus of points at which the inverse Green's function vanishes. Although the metal is globally isotropic, the excitations in the vicinity of a particular point on the Fermi surface have a highly anisotropic structure, as shown in Fig. 1: excitations at a momentum k_\perp perpendicular to the Fermi surface have a typical energy k_\perp^z , while excitations at a momentum k_\parallel parallel to the Fermi surface have a typical energy k_\parallel^{2z} ; here z is the dynamic critical exponent. In the present paper, we will show that the dispersion of the excitations parallel to the Fermi surface plays a more fundamental role in determining the value of the shear viscosity η . As a result Eq. (1) does not apply, and we find instead a divergence as $T \rightarrow 0$,

$$\eta/s \sim T^{-2/z}. \quad (2)$$

This surprising violation of (1) in an isotropic system can be traced directly to the presence of a Fermi surface. Our result implies that holographic duals of strange metals⁴⁵⁻⁵⁰ do not fully capture the Fermi surface structure. Instead, it appears that bulk quantum gravity corrections will be required to resurrect the Fermi surface in the holographic theories⁵¹⁻⁵³, and to obtain the result corresponding to Eq. (2).

Section II will present a review of scaling arguments which usually apply the conventional relation in Eq. (1). The dimensionally extended field theory for the quantum critical point will be presented in Section III. We will use this field theory to compute the 'optical' shear viscosity

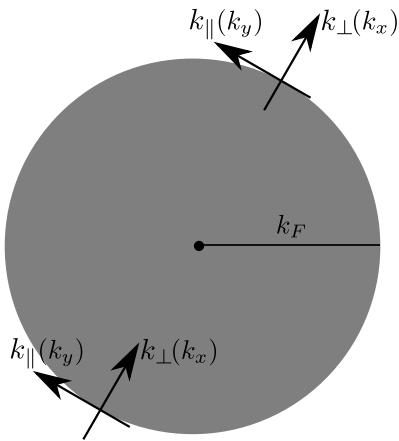


FIG. 1. Fermi surface and definition of the momentum components parallel (k_{\parallel}) and perpendicular (k_{\perp}) to the Fermi surface at the two Fermi surface patches in which the low-energy field theory is defined.

(*i.e.* the viscosity at frequencies $\omega \gg T$) in Section IV. We will then examine the usual DC viscosity (at frequencies $\omega \ll T$) in Section V.

II. SCALING ARGUMENTS

In studies so far of the thermodynamic and transport properties of strange metals, the anisotropy of the Fermi surface has had a specific consequence⁵⁴: the entropy density, and the electrical and thermal conductivities are dominated by the energy dispersion perpendicular to the Fermi surface, while the direction parallel to the Fermi surface mostly acts as a label which counts the total density of perpendicular excitations. Consequently, in scaling arguments we find a violation of hyperscaling: this is the property in which the entropy density of a d dimensional system scales as if it is in $d - \theta$ dimensions, with θ the violation of hyperscaling exponent. For a Fermi surface $\theta = d - 1$, because only the dispersion perpendicular to each point on the Fermi surface is important in the computation of the entropy. Recent work has shown⁵⁴ that similar arguments also correctly determine the electrical conductivity and entropy density.

We now review the general scaling arguments for the universality of η/s . The entropy density invariably scales as a density, and so has scaling dimension d . From the arguments just presented above, with the violation of hyperscaling in the presence of a Fermi surface, the entropy density s should have scaling dimension $d - \theta$, and so

$$s \sim T^{(d-\theta)/z}; \quad (3)$$

this was confirmed by computations in⁵⁴. Similar arguments apply to the optical conductivity $\sigma_Q(\omega)$, where ω is a frequency; naively, the conductivity has scaling dimension $d - 2$, and so we can expect that in the presence of a Fermi surface, the dimension will be $d - \theta - 2$. The

computation in⁵⁴ shows that this is indeed the case, and we have

$$\sigma_Q \sim T^{(d-2-\theta)/z} \Upsilon(\omega/T), \quad (4)$$

where Υ is a scaling function.

In an isotropic system that obeys hyperscaling, we can read off the scaling dimension of the stress tensor from its definition⁵⁵,

$$T_{\mu\nu} = \sum_n \left(\frac{\delta \mathcal{L}}{\delta(\partial_\mu \zeta_n)} \partial_\nu \zeta_n - \partial_\mu \frac{\delta \mathcal{L}}{\delta(\partial_\mu^2 \zeta_n)} \partial_\nu \zeta_n \right) - \delta_{\mu\nu} \mathcal{L}, \quad (5)$$

where ζ_n denotes all the fields in the theory and \mathcal{L} the Lagrangian density. It follows that the spatial components have the same scaling dimension as the Lagrangian density, $[T_{ij}] = d + z$, and that the mixed temporal-spatial components have scaling dimension $[T_{0i}] = d + 1$. Inserting these scaling dimensions into the Euler equation,

$$\partial_t p_\alpha = \partial_\beta T_{\alpha\beta}, \quad (6)$$

where p_α are the components of the momentum operator, yields consistent results. We thus obtain

$$[T_{xy}] = d + z \quad (7)$$

in the presence of hyperscaling. Kubo's formula for the frequency-dependent shear viscosity reads^{29,30},

$$\text{Re } \eta(\omega) = \lim_{\mathbf{q} \rightarrow 0} \omega^{-1} \text{Im } \chi_{T_{xy} T_{xy}}(\omega, \mathbf{q}), \quad (8)$$

where

$$\chi_{T_{xy} T_{xy}}(i\omega_n, \mathbf{q}) = \langle T_{xy}(i\omega_n, \mathbf{q}) T_{xy}(-i\omega_n, -\mathbf{q}) \rangle \quad (9)$$

is the autocorrelation function of the xy -component of the stress tensor T . Its scaling dimension is

$$[\eta] = -z - d - z + 2[T_{xy}] = d \quad (10)$$

and the d.c. shear viscosity is given by $\eta = \lim_{\omega \rightarrow 0} \eta(\omega)$. This is the same scaling dimension as for the entropy density above. With the violation of hyperscaling in the presence of a Fermi surface, the examples of the entropy density and the optical conductivity above suggest that η should scale just like s in Eq. (3), and hence Eq. (1) should apply. Our computations in this paper show that this is not true, and the Fermi surface leads to behavior genuinely different both from naive scaling assumptions, and from holographic examples: the T dependence of η is such that Eq. (2) holds.

III. FIELD THEORY

We now recall the field theory which allow us to formulate a systematic and controlled renormalization group analysis using a convenient dimensional regularization method. Moreover, this method fully preserves a two-dimensional Fermi surface with anisotropic dispersion in

the vicinity of every point on the Fermi surface, and these features are crucial for our results. We will discuss the field theory for the Ising-nematic critical point, but sim-

ilar field theories and results also apply to the problem of a Fermi surface coupled to a gauge field, or to other long-wavelength order parameters³⁷.

We consider a theory of fermions, ψ , in $(2+1)$ dimensions which are coupled to a critical boson, Φ ,

$$S(\bar{\psi}, \psi, \Phi) = \sum_{s=\pm} \sum_{j=1}^N \int \frac{d^3k}{(2\pi)^3} \bar{\psi}_{sj}^\dagger(k) (ik_0 + sk_x + k_y^2) \tilde{\psi}_{sj}(k) + \frac{1}{2} \int \frac{d^3k}{(2\pi)^3} (k_0^2 + k_x^2 + k_y^2) \Phi(-k) \Phi(k) \\ + \frac{e}{\sqrt{N}} \sum_{s=\pm} \sum_{j=1}^N \int \frac{d^3k}{(2\pi)^3} \int \frac{d^3q}{(2\pi)^3} \lambda_s \Phi(q) \tilde{\psi}_{sj}^\dagger(k+q) \tilde{\psi}_{sj}(k), \quad (11)$$

where e is the fermion-boson coupling constant, $s = \pm 1$ labels the two Fermi surface patches, N is the number of fermionic flavors and λ_s equals 1 (s) for the Ising-nematic critical point (fermions coupled to a $U(1)$ gauge field). This model has been studied by many authors, including Refs. 37 and 38. In the following, we restrict ourselves to the Ising-nematic critical point and set $\lambda_s = 1$.

This model can be studied in a controlled way using the dimensional regularization scheme proposed by Dali-dovich and Lee³⁸. Increasing the codimension of the Fermi surface by introducing auxiliary time-like directions, the dimensionally regularized action in $(d+1)$ dimensions reads

$$S(\bar{\psi}, \psi, \Phi) = \sum_{j=1}^N \int \frac{d^{d+1}k}{(2\pi)^{d+1}} \bar{\psi}_j(k) [i\mathbf{\Gamma} \cdot \mathbf{K} + i\gamma_x \delta_k] \psi_j(k) + \frac{1}{2} \int \frac{d^{d+1}q}{(2\pi)^{d+1}} [\mathbf{Q}^2 + q_x^2 + q_y^2] \Phi(-q) \Phi(q) \\ + \frac{ie}{\sqrt{N}} \sqrt{d-1} \sum_{j=1}^N \int \frac{d^{d+1}k}{(2\pi)^{d+1}} \int \frac{d^{d+1}q}{(2\pi)^{d+1}} \Phi(q) \bar{\psi}_j(k+q) \gamma_x \psi_j(k), \quad (12)$$

where $\mathbf{K} = (k_0, k_1, \dots, k_{d-2})$ collects the physical and $(d-2)$ auxiliary frequency variables. We introduced the spinor notation

$$\psi_j(k) = \left(\tilde{\psi}_{+,j}(k), \tilde{\psi}_{-,j}^\dagger(-k) \right)^T \quad \bar{\psi}_j(k) = \psi_j^\dagger(k) \gamma_0 \quad (13)$$

and defined the gamma matrices as $\gamma_0 = \sigma_y$ and $\gamma_x = \sigma_x$ for the spatial and as $\mathbf{\Gamma} = (\gamma_0, \gamma_1, \dots, \gamma_{d-2})$ for the time-like directions. Within a patch, we choose k_x (k_y) perpendicular (parallel) to the Fermi surface, as shown in Fig. 1. The dispersion in the spatial plane containing the Fermi surface is δ_k , while the full dispersion is ε_k with

$$\delta_k = k_x + \sqrt{d-1} k_y^2, \quad \varepsilon_k = \left(\delta_k^2 + \sum_{i=1}^{d-2} k_i^2 \right)^{1/2}. \quad (14)$$

Note the line of zero energy excitations in the plane $k_i = 0$ which represents a patch on the Fermi surface in Fig. 1, and the relativistic dispersion along the k_i directions.

Rescaling momenta as

$$\mathbf{K} = b^{-1} \mathbf{K}' \quad k_x = b^{-1} k'_x \quad k_y = b^{-1/2} k'_y, \quad (15)$$

the fermionic quadratic part of the action and the contribution $\sim q_y^2$ in the bosonic quadratic part of the action are invariant under rescaling if fields are scaled as

$$\psi_j(k) = b^{d/2+3/4} \psi'_j(k') \quad \Phi(k) = b^{d/2+3/4} \Phi'(k') \quad (16)$$

The terms proportional to \mathbf{Q}^2 and q_x^2 in the bosonic quadratic part are irrelevant under this rescaling. The coupling scales as

$$e' = eb^{\frac{1}{2}(5/2-d)}, \quad (17)$$

identifying $d = 5/2$ as the upper critical dimension. It is irrelevant for $d > 5/2$ and relevant for $d < 5/2$. This allows to access non-Fermi liquid physics perturbatively by using $\epsilon = 5/2 - d$ as expansion parameter.

Keeping only marginal terms, the ansatz for the local field theory reads

$$S(\bar{\psi}, \psi, \Phi) = \sum_{j=1}^N \int \frac{d^{d+1}k}{(2\pi)^{d+1}} \bar{\psi}_j(k) [i\mathbf{\Gamma} \cdot \mathbf{K} + i\gamma_x \delta_k] \psi_j(k) + \frac{1}{2} \int \frac{d^{d+1}q}{(2\pi)^{d+1}} q_y^2 \Phi(-q) \Phi(q) \\ + \frac{ie\mu^{\epsilon/2}}{\sqrt{N}} \sqrt{d-1} \sum_{j=1}^N \int \frac{d^{d+1}k}{(2\pi)^{d+1}} \int \frac{d^{d+1}q}{(2\pi)^{d+1}} \Phi(q) \bar{\psi}_j(k+q) \gamma_x \psi_j(k), \quad (18)$$

where we introduced the momentum scale μ in order to make the coupling e dimensionless. Perturbative corrections to this action at one-loop level reintroduce dynamics for the bosonic field. The $\epsilon = 5/2 - d$ expansion allows us to make a renormalized perturbative computation in the dimensionless coupling e . Note that this is not equivalent to a simple $1/N$ expansion, which breaks down at the Ising-nematic QCP³⁷, and that the expansion parameter is $\frac{e^{4/3}}{N}$ ³⁸.

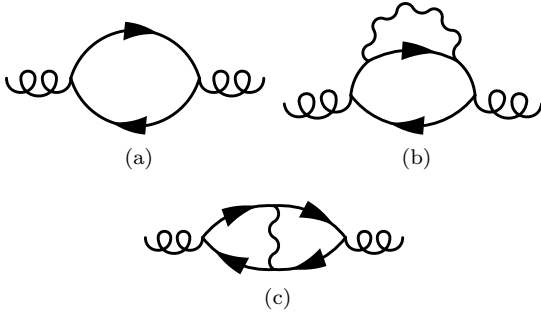


FIG. 2. Feynman diagrams yielding the renormalization of the scaling behavior of the viscosity at lowest order in ϵ : (a) One-loop contribution, (b) self-energy correction and (c) vertex correction. Lines represent fermionic propagators, wiggly lines bosonic propagators and curly lines the stress tensor.

IV. OPTICAL SHEAR VISCOSITY

In the following, we focus on the ‘optical’ shear viscosity, evaluated at frequencies $\omega \gg T$. Its evaluation is simpler than that for the d.c. viscosity, $\omega \ll T$, which will be considered in Section V.

For the Ising-nematic QCP the xy -component of the stress tensor is proportional to the y -component of the ‘chiral’ current operator,

$$T_{xy}(q) = i \sum_{j=1}^N \int_k (k_y + \frac{q_y}{2}) \bar{\psi}_j(k+q) \gamma_x \psi_j(k) \\ = \frac{1}{2\sqrt{d-1}} J_y(q). \quad (19)$$

where $\int_k = \int \frac{dk_x}{2\pi} \int \frac{dk_y}{2\pi} \int \frac{d^{d-1}K}{(2\pi)^{d-1}}$. Note that the x - and y -components of the chiral current contain the same gamma matrix.

The Feynman diagrams describing the renormalization of the scaling behavior of the viscosity at lowest order in ϵ are shown in Fig. 2.

At one-loop level, the stress tensor correlator is given

by

$$\langle T_{xy}(q) T_{xy}(-q) \rangle_{1\text{Loop}} = \\ = N \int_k (k_y + q_y/2)^2 \text{tr}(\gamma_x G_0(k+q) \gamma_x G_0(k)) \quad (20)$$

where

$$G_0(k) = \frac{\mathbf{\Gamma} \cdot \mathbf{K} + \gamma_x \delta_k}{i(\mathbf{K}^2 + \delta_k^2)} \quad (21)$$

is the bare fermionic Green’s function. Specializing to $q = \omega \mathbf{e}_0$,

$$\langle T_{xy} T_{xy} \rangle_{1\text{Loop}}(i\omega) = \\ = -2N \int \frac{d^{d+1}k}{(2\pi)^{d+1}} k_y^2 \frac{\delta_k^2 - \mathbf{K} \cdot (\mathbf{K} + \mathbf{Q})}{(\mathbf{K}^2 + \delta_k^2)((\mathbf{K} + \mathbf{Q})^2 + \delta_k^2)}, \quad (22)$$

where $\mathbf{Q} = \omega \mathbf{e}_0$. The further evaluation parallels that of the optical conductivity⁵⁴. Shifting $k_x \rightarrow k_x - \sqrt{d-1}k_y^2$ eliminates k_y from the integrand except in the prefactor arising from the stress tensor, yielding

$$\langle T_{xy} T_{xy} \rangle_{1\text{Loop}}(i\omega) = \\ -2N \int \frac{dk_y}{2\pi} k_y^2 \int \frac{dk_x}{2\pi} \int \frac{d^{d-1}K}{(2\pi)^{d-1}} \frac{k_x^2 - \mathbf{K} \cdot (\mathbf{K} + \mathbf{Q})}{(\mathbf{K}^2 + k_x^2)((\mathbf{K} + \mathbf{Q})^2 + k_x^2)} \\ = -2N \int \frac{dk_y}{2\pi} k_y^2 I_{1\text{loop}}(\mathbf{Q}). \quad (23)$$

Introducing Feynman parameters, completing squares in the denominator and shifting $\mathbf{K} \rightarrow \mathbf{K} - (1-x)\mathbf{Q}$, we obtain

$$I_{1\text{loop}}(\mathbf{Q}) = \\ \int \frac{d^{d-1}K}{(2\pi)^{d-1}} \int \frac{dp}{(2\pi)} \int_0^1 dx \frac{p^2 - \mathbf{K}^2 + x(1-x)\mathbf{Q}^2}{[\mathbf{K}^2 + p^2 + x(1-x)\mathbf{Q}^2]^2} \\ = \frac{\pi S_{d-1}}{(2\pi)^d} \int_0^\infty dk k^{d-2} \int_0^1 dx \frac{x(1-x)\mathbf{Q}^2}{[k^2 + x(1-x)\mathbf{Q}^2]^{3/2}} \\ = \frac{S_{d-1}}{(2\pi)^d} \sqrt{\pi} \Gamma(2-d/2) \frac{\Gamma(\frac{d-1}{2})\Gamma(d/2)^2}{\Gamma(d)} |\mathbf{Q}|^{d-2} \quad (24)$$

($S_d = 2\pi^{d/2}/\Gamma(d/2)$). For $d = 5/2 - \epsilon$, the one-loop result for the stress tensor autocorrelation function thus reads

$$\langle T_{xy} T_{xy} \rangle_{\text{1loop}}(i\omega) = -N u_{\text{1Loop},\epsilon} \int \frac{dk_y}{2\pi} k_y^2 |\omega|^{1/2-\epsilon}, \quad (25)$$

where

$$u_{\text{1Loop},\epsilon} = \frac{2^{\epsilon-1/2} \Gamma(\frac{3+2\epsilon}{4}) \Gamma(\frac{5-2\epsilon}{4})^2}{\sqrt{\pi} 5/2-\epsilon \Gamma(\frac{5-2\epsilon}{2})}. \quad (26)$$

The momentum parallel to the Fermi surface, k_y , does not scale due to the emergent rotational symmetry³⁷ of the low-energy field theory. The latter restricts the momentum dependence of the fermionic and bosonic propagator to $G(\mathbf{K}, k_x, k_y) = G(\mathbf{K}, \delta_k)$ and $D(\mathbf{Q}, q_x, q_y) = D(\mathbf{Q}, q_y)$, respectively, which allows to eliminate k_y from the integrand by shifting k_x . The k_y -integral is cut off by the Fermi surface curvature. As a consequence, the result (25) differs from the current-current correlation function only by the fact that $\int_{k_y} k_y^2$ appears instead of \int_{k_y} ⁵⁴. Importantly, both results have the same dependence on frequency.

The two-loop self-energy correction to the optical viscosity is given by

$$\begin{aligned} \langle T_{xy} T_{xy} \rangle_{\text{SE}}(i\omega) &= 2N \int_k (k_y + q_y/2)^2 \\ &\times \text{tr} \left(\gamma_x G_0(k+q) \gamma_x G_0(k) \Sigma_1(k) G_0(k) \right), \end{aligned} \quad (27)$$

where

$$\Sigma_1(k) = -i(\Gamma \cdot \mathbf{Q}) \frac{e^{4/3}}{N} \left(\frac{\mu}{|\mathbf{Q}|} \right)^{2\epsilon/3} u_{\Sigma,0} \epsilon^{-1} + \mathcal{O}(\epsilon^0) \quad (28)$$

is the one-loop fermionic self-energy³⁸ ($u_{\Sigma,0} = (2 \cdot 6^{1/3} \pi)^{-1}$). We obtain

$$\langle T_{xy} T_{xy} \rangle_{\text{SE}}(i\omega) = e^{4/3} \epsilon^{-1} \int_{k_y} k_y^2 |\omega|^{1/2-\epsilon} \left(\frac{\mu}{|\omega|} \right)^{2\epsilon/3} a_{\Sigma,0}, \quad (29)$$

where $a_{\Sigma,0} = u_{\text{1Loop},0} u_{\Sigma,0}$, after evaluation of the integrals as described in Appendix A. The dependence on frequency is the same as in the self-energy correction to the current-current correlation function⁵⁴.

The two-loop vertex correction is given by

$$\begin{aligned} \langle T_{xy} T_{xy} \rangle_{\text{VC}}(i\omega) &= -iN \int_k (k_y + q_y/2) \\ &\times \text{tr} \left(\gamma_x G_0(k+q) \Gamma_{xy,1}(k, q) G_0(k) \right), \end{aligned} \quad (30)$$

where $\Gamma_{xy,1}$ is the one-loop correction to the stress-tensor. Ward identities due to the conservation of the chiral current imply that the vertex correction to the stress tensor correlation function does not have a pole in ϵ^{-1} , as for the optical conductivity^{38,54}. At lowest order in ϵ , we thus obtain

$$\begin{aligned} \langle T_{xy} T_{xy} \rangle(i\omega) &= -N \int_{k_y} k_y^2 u_{\text{1Loop},0} \\ &\times |\omega|^{1/2-\epsilon} \left\{ 1 - \frac{e^{4/3}}{N\epsilon} \left(\frac{\mu}{|\omega|} \right)^{2\epsilon/3} u_{\Sigma,0} \right\} + \dots \end{aligned} \quad (31)$$

for the correlator of the stress tensor. Evaluation of the coupling $e^{4/3}/N$ at the fixed point using the β function in $\mathcal{O}(\epsilon)$ ³⁸,

$$\left(\frac{e^{4/3}}{N} \right)^* = u_{\Sigma,0}^{-1} \epsilon, \quad (32)$$

and resummation of the frequency dependence yields $\langle T_{xy} T_{xy} \rangle(i\omega) \sim |\omega|^{1/2-\epsilon/3}$ for the correlator and

$$\eta(\omega) \sim \omega^{-1/2-\epsilon/3} \quad (33)$$

for the optical shear viscosity. Repeating the scaling arguments as described in Section II for two spatial dimensions, one time dimension and $1/2 - \epsilon$ auxiliary time dimensions, the optical shear viscosity is expected to scale as

$$\eta(\omega) \sim \omega^{(d+(1/2-\epsilon)z-\theta_\eta)/z}, \quad (34)$$

where θ_η is a hyperscaling violation exponent. The result in Eq. (33) corresponds to $\theta_\eta = 3$, and thus $\theta_\eta \neq \theta$. The origin of this breakdown of the scaling expectation is the k_y^2 factor in Eq. (31), which is dominated by contributions near the cutoff.

Instead, the result in Eq. (33) suggests that the viscosity scales like a conductivity. For the conductivity, the arguments in Section II imply that for the present dimensionally extended system, the scaling law in Eq. (4) is modified to

$$\sigma(\omega) \sim \omega^{(d+(1/2-\epsilon)z-\theta-2)/z}, \quad (35)$$

using the values $d = 2$, $\theta = 1$, and $z = 3/(3 - 2\epsilon)$, this agrees with Eq. (33). The Ward identity analysis in Appendix B shows that the identity of the scaling between the viscosity and the conductivity holds to all orders.

In the above computation, we considered the contributions to the optical viscosity from two patches on the Fermi surface. In Appendix C, we show that the scaling is the same if contributions from the full Fermi surface are taken into account. Moreover, by using Ward identities we trace the above conclusion back to the emergent rotation invariance of the low energy field theory, or equivalently to the fact that the Fermi surface curvature does not flow.

Given the scaling of entropy in the present system

$$s \sim T^{(d+(1/2-\epsilon)z-\theta)/z}, \quad (36)$$

our main result in Eq. (2) would follow from Eq. (35) provided the viscosity scaled in the same manner with T in the regime $\omega \ll T$, as it does with ω in $\omega \gg T$. We will turn to this important question in the following section.

V. BOLTZMANN EQUATION AND DC VISCOSITY

This section presents a Boltzmann equation analysis which shows that ω/T scaling applies, and that the ω -dependent results above can be extended to the d.c. viscosity with $\omega \rightarrow T$. We set $N = 1$ in this section for

convenience. The DC viscosity may be derived in linear response by applying a static source that couples linearly to T_{xy} , which is equivalent to applying a static source that couples linearly to J_y for the fermion contribution, i.e. a chiral electric field.

Since our action is invariant under inversion for the full Fermi surface, i.e.

$$\tilde{\psi}_s(k_0, k_x, k_y) = \tilde{\psi}_{\bar{s}}(k_0, -k_x, -k_y), \quad (37)$$

and this leaves J_y invariant but inverts the total momentum $P_i \rightarrow -P_i$, the chiral current has zero overlap with the conserved total momentum, i.e.

$$\chi_{J_y P_i} \equiv \int_0^{1/T} \langle J_y(\tau) P_i(0) \rangle = 0. \quad (38)$$

Thus, the DC chiral conductivities and hence the DC viscosities are finite and can be determined using the Boltzmann equation. Fig. 3 illustrates how chiral currents can be excited without changing the total momentum of the system. This requires oppositely directed electric fields to be applied to the two patches.

The kinetic part of the fermion Hamiltonian in the

dimensionally regularized theory may be diagonalized as

$$\begin{aligned} H_f^0 &= \int \frac{d^d \mathbf{k}}{(2\pi)^d} \bar{\psi}(\mathbf{k}) [i\bar{\Gamma} \cdot \bar{\mathbf{K}} + i\gamma_x \delta_k] \psi(\mathbf{k}) \\ &= \sum_{m=\pm} \int \frac{d^d \mathbf{k}}{(2\pi)^d} m \lambda_m^\dagger(\mathbf{k}) \xi(\mathbf{k}) \lambda_m(\mathbf{k}), \end{aligned} \quad (39)$$

where we use $\mathbf{k} = (k_x, k_y, \bar{\mathbf{K}})$, $\bar{\mathbf{K}} = (k_1, \dots, k_{d-2})$ and $\bar{\Gamma} = (\gamma_1, \dots, \gamma_{d-2})$, with the dispersion

$$\xi(\mathbf{k}) = (\bar{\mathbf{K}}^2 + \delta_k^2)^{1/2}. \quad (40)$$

The y -component of the chiral current density becomes

$$J_y = \left(\sum_{m=\pm} \int \frac{d^d \mathbf{k}}{(2\pi)^d} \frac{m \delta_k \partial_{k_y} \delta_k}{\sqrt{\bar{\mathbf{K}}^2 + \delta_k^2}} \lambda_m^\dagger(\mathbf{k}) \lambda_m(\mathbf{k}) \right) + J_y^{II}, \quad (41)$$

where J_y^{II} contains particle-hole terms $\lambda_+^\dagger \lambda_-$, $\lambda_-^\dagger \lambda_+$ that are unimportant for transport in the DC regime of interest^{13,56}. Defining the non-equilibrium on-shell fermion distribution functions

$$f_f^m(t, \mathbf{k}) = \langle \lambda_m^\dagger(t, \mathbf{k}) \lambda_m(t, \mathbf{k}) \rangle, \quad (42)$$

and the non-equilibrium off-shell boson distribution function $f_b(t, \mathbf{q}, \Omega)$, we can write down the following collision equations in presence of an applied chiral electric field \mathbf{E} ^{56–58}:

$$\begin{aligned} \left(\frac{\partial}{\partial t} + \mathbf{E} \cdot \frac{\partial}{\partial \mathbf{p}} \right) f_f^m(\mathbf{p}, t) &= -e^2 \mu^\epsilon \sum_{m'=\pm} \int \frac{d^d \mathbf{q}}{(2\pi)^d} M_{mm'}(\mathbf{p}, \mathbf{q}) \text{Im} [D^R(\mathbf{p} - \mathbf{q}, m\xi(\mathbf{p}) - m'\xi(\mathbf{q}))] \\ &\times \left\{ f_f^m(t, \mathbf{p})(1 - f_f^{m'}(t, \mathbf{q})) + f_b(t, \mathbf{p} - \mathbf{q}, m\xi(\mathbf{p}) - m'\xi(\mathbf{q})) (f_f^m(t, \mathbf{p}) - f_f^{m'}(t, \mathbf{q})) \right\}, \end{aligned} \quad (43)$$

$$\begin{aligned} \left[\frac{\partial}{\partial \Omega} (2\Omega^2 - \text{Re}[\Sigma_b^R(t, \mathbf{q}, \Omega)]) \frac{\partial}{\partial t} + \frac{\partial \text{Re}[\Sigma_b^R(t, \mathbf{q}, \Omega)]}{\partial t} \frac{\partial}{\partial \Omega} \right] f_b(t, \mathbf{q}, \Omega) &= \\ 4\pi e^2 \mu^\epsilon \sum_{m, m'=\pm} \int \frac{d^d \mathbf{k}}{(2\pi)^d} M_{mm'}(\mathbf{k} + \mathbf{q}, \mathbf{k}) \delta(m\xi(\mathbf{k} + \mathbf{q}) - m'\xi(\mathbf{k}) - \Omega) &\left[f_f^m(t, \mathbf{k} + \mathbf{q})(1 - f_f^{m'}(t, \mathbf{k})) \right. \\ \left. + f_b(t, \mathbf{q}, \Omega)(f_f^m(t, \mathbf{k} + \mathbf{q}) - f_f^{m'}(t, \mathbf{k})) \right], \end{aligned} \quad (44)$$

where the interaction matrix elements are

$$M_{mm'}(\mathbf{p}, \mathbf{q}) = \frac{1}{2} \left(1 + mm' \frac{\delta_p \delta_q - \bar{\mathbf{P}} \cdot \bar{\mathbf{Q}}}{\xi(\mathbf{p}) \xi(\mathbf{q})} \right) \quad (45)$$

(Note that $M_{++} = M_{--}$, $M_{+-} = M_{-+}$ and $M_{mm'}(\mathbf{p}, \mathbf{q}) = M_{mm'}(\mathbf{q}, \mathbf{p})$), and

$$D^R(\mathbf{k}, \omega) = \frac{|k_y|}{|k_y|^3 + \beta_d e^2 \mu^\epsilon (\bar{\mathbf{K}}^2 - \omega^2)^{(d-1)/2}}, \quad (46)$$

where β_d depends only on d and is free of poles in ϵ ³⁸. The additional self-energy component appearing in the boson

collision equation is given by⁵⁸

$$\text{Re}[\Sigma_b^R(t, \mathbf{q}, \Omega)] = -2e^2\mu^\epsilon \sum_{mm'=\pm} \int \frac{d^d\mathbf{k}}{(2\pi)^d} M_{mm'}(\mathbf{k}, \mathbf{k} + \mathbf{q}) \frac{f_f^{m'}(t, \mathbf{k} + \mathbf{q}) - f_f^m(t, \mathbf{k})}{m\xi(\mathbf{k}) - m'\xi(\mathbf{k} + \mathbf{q}) + \Omega}. \quad (47)$$

Both collision integrals vanish regardless of what D^R is when the equilibrium distributions are used due to the identity

$$n_f(x)(1 - n_f(y)) + n_b(x - y)(n_f(x) - n_f(y)) = 0. \quad (48)$$

We parameterize the deviations of the distributions from equilibrium in frequency space

$$\begin{aligned} f_f^m(\omega, \mathbf{p}) &= 2\pi\delta(\omega)n_f(m\xi(\mathbf{p})) - Tn'_f(\xi(\mathbf{p}))\varphi^m(\omega, \delta_p, \bar{\mathbf{P}})\mathbf{E}(\omega) \cdot \nabla_{\mathbf{p}}\xi(\mathbf{p}), \\ f_b(\omega, \mathbf{q}, \Omega) &= 2\pi\delta(\omega)n_b(\Omega) + u(\omega, \mathbf{q}, \Omega)|\mathbf{E}(\omega)|. \end{aligned} \quad (49)$$

Using these, we linearize the collision equations with $\mathbf{E} = E_y\hat{e}_y$ as we are interested in J_y . In the DC limit, we obtain (since $\lim_{\omega \rightarrow 0}(-i\omega + 0^+)\varphi^m(\omega, \delta_p, \bar{\mathbf{P}})$ and $\lim_{\omega \rightarrow 0}(-i\omega + 0^+)u(\omega, \mathbf{q}, \Omega)$ are expected to vanish in the presence of interactions)

$$\begin{aligned} \frac{2m\delta_p\sqrt{d-1}p_y}{\xi(\mathbf{p})}n'_f(\xi(\mathbf{p})) &= -e^2\mu^\epsilon \sum_{m'=\pm} \int \frac{d^d\mathbf{q}}{(2\pi)^d} M_{mm'}(\mathbf{p}, \mathbf{q})\text{Im}[D^R(\mathbf{p} - \mathbf{q}, m\xi(\mathbf{p}) - m'\xi(\mathbf{q}))] \\ &\times \left\{ \frac{2\delta_q\sqrt{d-1}q_y}{\xi(\mathbf{q})}\varphi^{m'}(\delta_q, \bar{\mathbf{Q}})Tn'_f(\xi(\mathbf{q}))n_f(m\xi(\mathbf{p})) - \frac{2\delta_p\sqrt{d-1}p_y}{\xi(\mathbf{p})}\varphi^m(\delta_p, \bar{\mathbf{P}})Tn'_f(\xi(\mathbf{p}))(1 - n_f(m'\xi(\mathbf{q}))) \right. \\ &+ n_b(m\xi(\mathbf{p}) - m'\xi(\mathbf{q})) \left(\frac{2\delta_q\sqrt{d-1}q_y}{\xi(\mathbf{q})}\varphi^{m'}(\delta_q, \bar{\mathbf{Q}})Tn'_f(\xi(\mathbf{q})) - \frac{2\delta_p\sqrt{d-1}p_y}{\xi(\mathbf{p})}\varphi^m(\delta_p, \bar{\mathbf{P}})Tn'_f(\xi(\mathbf{p})) \right) \\ &\left. + \text{sgn}(E_y)u(\mathbf{p} - \mathbf{q}, m\xi(\mathbf{p}) - m'\xi(\mathbf{q}))(n_f(m\xi(\mathbf{p})) - n_f(m'\xi(\mathbf{q}))) \right\}. \end{aligned} \quad (50)$$

where we have suppressed the now zero frequency argument on the φ 's and u 's. For the boson collision equation we obtain

$$\begin{aligned} u(\mathbf{q}, \Omega) &= \text{sgn}(E_y) \frac{I_1[\varphi, \mathbf{q}, \Omega]}{I_2(\mathbf{q}, \Omega)}, \\ I_1[\varphi, \mathbf{q}, \Omega] &= 4\pi e^2\mu^\epsilon \sum_{mm'=\pm} \int \frac{d^d\mathbf{k}}{(2\pi)^d} M_{mm'}(\mathbf{k} + \mathbf{q}, \mathbf{k})\delta(m\xi(\mathbf{k} + \mathbf{q}) - m'\xi(\mathbf{k}) - \Omega) \\ &\times \left[\frac{2\delta_k\sqrt{d-1}k_y}{\xi(\mathbf{k})}\varphi^{m'}(\delta_k, \bar{\mathbf{K}})Tn'_f(\xi(\mathbf{k}))n_f(m\xi(\mathbf{k} + \mathbf{q})) \right. \\ &- \left. \frac{2\delta_{k+q}\sqrt{d-1}(k_y + q_y)}{\xi(\mathbf{k} + \mathbf{q})}\varphi^m(\delta_{k+q}, \bar{\mathbf{K}} + \bar{\mathbf{Q}})Tn'_f(\xi(\mathbf{k} + \mathbf{q}))(1 - n_f(m'\xi(\mathbf{k}))) \right] \\ &+ n_b(\Omega) \left\{ \frac{2\delta_k\sqrt{d-1}k_y}{\xi(\mathbf{k})}\varphi^{m'}(\delta_k, \bar{\mathbf{K}})Tn'_f(\xi(\mathbf{k})) - 2\frac{\delta_{k+q}\sqrt{d-1}(k_y + q_y)}{\xi(\mathbf{k} + \mathbf{q})}\varphi^m(\delta_{k+q}, \bar{\mathbf{K}} + \bar{\mathbf{Q}})Tn'_f(\xi(\mathbf{k} + \mathbf{q})) \right\}, \\ I_2(\mathbf{q}, \Omega) &= -4\pi e^2\mu^\epsilon \sum_{mm'=\pm} \int \frac{d^d\mathbf{k}}{(2\pi)^d} M_{mm'}(\mathbf{k} + \mathbf{q}, \mathbf{k})\delta(m\xi(\mathbf{k} + \mathbf{q}) - m'\xi(\mathbf{k}) - \Omega) \\ &\times \left\{ n_f(m\xi(\mathbf{k} + \mathbf{q})) - n_f(m'\xi(\mathbf{k})) \right\}. \end{aligned} \quad (51)$$

Since the driving term for the fermions in Eq. (44) is of opposite signs for the + and - quasiparticles, we expect $\varphi^m(\delta_p, \bar{\mathbf{P}}) = m\varphi(\delta_p, \bar{\mathbf{P}})$. Then, using the properties of the matrix elements M noted previously and that $n_{f,b}(x) + n_{f,b}(-x) = \pm 1$, one can see that u is an odd function of Ω and hence that the same $\varphi(\delta_k, \bar{\mathbf{K}})$ can be used to solve the collision equations for both branches of quasiparticles.

In the (convergent) boson collision integrals in Eq. (51), we shift $k_x \rightarrow k_x - \sqrt{d-1}k_y^2$ and integrate over k_y . In the (also convergent) fermion collision integral Eq. (50), after inserting u derived from the boson collision equation we shift $q_x \rightarrow q_x - \sqrt{d-1}q_y^2$ followed by $q_y \rightarrow q_y + p_y$, and then integrate out q_y after dividing through by $2\sqrt{d-1}p_y$.

Terms that are odd in q_y drop out, and we are left with

$$\begin{aligned}
\frac{m\delta_p}{\xi(\mathbf{p})} n'_f(\xi(\mathbf{p})) &= -\frac{e^2\mu^\epsilon}{2} \sum_{m'=\pm} \int \frac{d^{d-1}\mathbf{q}}{(2\pi)^d} \left(1 + mm' \frac{\delta_p q_x - \bar{\mathbf{P}} \cdot \bar{\mathbf{Q}}}{\xi(\mathbf{p}) \sqrt{\bar{\mathbf{Q}}^2 + q_x^2}} \right) \\
&\times \text{Im} \left[\frac{4\pi}{\sqrt{27}} \left(\beta_d e^2 \mu^\epsilon \left((\bar{\mathbf{P}} - \bar{\mathbf{Q}})^2 - \left(m\xi(\mathbf{p}) - m' \sqrt{\bar{\mathbf{Q}}^2 + q_x^2} \right)^2 \right)^{(d-1)/2} \right)^{-1/3} \right] \\
&\times \left\{ \frac{q_x}{\sqrt{\bar{\mathbf{Q}}^2 + q_x^2}} \varphi^{m'}(q_x, \bar{\mathbf{Q}}) T n'_f \left(\sqrt{\bar{\mathbf{Q}}^2 + q_x^2} \right) n_f(m\xi(\mathbf{p})) \right. \\
&- \frac{\delta_p}{\xi(\mathbf{p})} \varphi^m(\delta_p, \bar{\mathbf{P}}) T n'_f(\xi(\mathbf{p})) \left(1 - n_f \left(m' \sqrt{\bar{\mathbf{Q}}^2 + q_x^2} \right) \right) \\
&+ n_b \left(m\xi(\mathbf{p}) - m' \sqrt{\bar{\mathbf{Q}}^2 + q_x^2} \right) \left(\frac{q_x}{\sqrt{\bar{\mathbf{Q}}^2 + q_x^2}} \varphi^{m'}(q_x, \bar{\mathbf{Q}}) T n'_f \left(\sqrt{\bar{\mathbf{Q}}^2 + q_x^2} \right) - \frac{\delta_p}{\xi(\mathbf{p})} \varphi^m(\delta_p, \bar{\mathbf{P}}) T n'_f(\xi(\mathbf{p})) \right) \\
&\left. - \frac{H_1[\varphi, \bar{\mathbf{P}} - \bar{\mathbf{Q}}, m\xi(\mathbf{p}) - m' \sqrt{\bar{\mathbf{Q}}^2 + q_x^2}]}{H_2(\bar{\mathbf{P}} - \bar{\mathbf{Q}}, |m\xi(\mathbf{p}) - m' \sqrt{\bar{\mathbf{Q}}^2 + q_x^2}|)} \left(n_f(m\xi(\mathbf{p})) - n_f \left(m' \sqrt{\bar{\mathbf{Q}}^2 + q_x^2} \right) \right) \right\}, \tag{52}
\end{aligned}$$

where

$$\begin{aligned}
H_1[\varphi, \bar{\mathbf{Q}}, \Omega] &= \sum_{mm's} \int \frac{d^{d-1}\mathbf{k}}{(2\pi)^d} \frac{|m' \sqrt{\bar{\mathbf{K}}^2 + k_x^2} + \Omega| \Theta((m' \sqrt{\bar{\mathbf{K}}^2 + k_x^2} + \Omega)^2 - (\bar{\mathbf{K}} + \bar{\mathbf{Q}})^2)}{\left((m' \sqrt{\bar{\mathbf{K}}^2 + k_x^2} + \Omega)^2 - (\bar{\mathbf{K}} + \bar{\mathbf{Q}})^2 \right)^{1/2}} \\
&\times \left(1 + mm' \frac{s \left((m' \sqrt{\bar{\mathbf{K}}^2 + k_x^2} + \Omega)^2 - (\bar{\mathbf{K}} + \bar{\mathbf{Q}})^2 \right)^{1/2} k_x - (\bar{\mathbf{K}} + \bar{\mathbf{Q}}) \cdot \bar{\mathbf{K}}}{|m' \sqrt{\bar{\mathbf{K}}^2 + k_x^2} + \Omega| \sqrt{\bar{\mathbf{K}}^2 + k_x^2}} \right) \\
&\times \left[\varphi^m(s((m'(\bar{\mathbf{K}}^2 + k_x^2)^{1/2} + \Omega)^2 - (\bar{\mathbf{K}} + \bar{\mathbf{Q}})^2)^{1/2}, \bar{\mathbf{K}} + \bar{\mathbf{Q}}) \frac{s((m'(\bar{\mathbf{K}}^2 + k_x^2)^{1/2} + \Omega)^2 - (\bar{\mathbf{K}} + \bar{\mathbf{Q}})^2)^{1/2}}{|m' \sqrt{\bar{\mathbf{K}}^2 + k_x^2} + \Omega|} \right. \\
&\times T n'_f(m'(\bar{\mathbf{K}}^2 + k_x^2)^{1/2} + \Omega) \left\{ 1 - n_f(m'(\bar{\mathbf{K}}^2 + k_x^2)^{1/2}) + n_b(\Omega) \right\} \\
&\left. - \varphi^{m'}(k_x, \bar{\mathbf{K}}) \frac{k_x}{\sqrt{\bar{\mathbf{K}}^2 + k_x^2}} T n'_f(m'(\bar{\mathbf{K}}^2 + k_x^2)^{1/2}) \left\{ n_f(m'(\bar{\mathbf{K}}^2 + k_x^2)^{1/2} + \Omega) + n_b(\Omega) \right\} \right], \\
H_2(\bar{\mathbf{Q}}, \Omega) &= \sum_{mm's} \int \frac{d^{d-1}\mathbf{k}}{(2\pi)^d} \frac{|m' \sqrt{\bar{\mathbf{K}}^2 + k_x^2} + \Omega| \Theta((m' \sqrt{\bar{\mathbf{K}}^2 + k_x^2} + \Omega)^2 - (\bar{\mathbf{K}} + \bar{\mathbf{Q}})^2)}{\left((m' \sqrt{\bar{\mathbf{K}}^2 + k_x^2} + \Omega)^2 - (\bar{\mathbf{K}} + \bar{\mathbf{Q}})^2 \right)^{1/2}} \\
&\times \left(1 + mm' \frac{s \left((m' \sqrt{\bar{\mathbf{K}}^2 + k_x^2} + \Omega)^2 - (\bar{\mathbf{K}} + \bar{\mathbf{Q}})^2 \right)^{1/2} k_x - (\bar{\mathbf{K}} + \bar{\mathbf{Q}}) \cdot \bar{\mathbf{K}}}{|m' \sqrt{\bar{\mathbf{K}}^2 + k_x^2} + \Omega| \sqrt{\bar{\mathbf{K}}^2 + k_x^2}} \right) \\
&\times \left\{ n_f \left(m' \sqrt{\bar{\mathbf{K}}^2 + k_x^2} + \Omega \right) - n_f \left(m' \sqrt{\bar{\mathbf{K}}^2 + k_x^2} \right) \right\}. \tag{53}
\end{aligned}$$

If we choose $\varphi^m(\delta_p, \bar{\mathbf{P}}) = \varphi(\delta_p, \bar{\mathbf{P}})$ with $\varphi(\delta_p, \bar{\mathbf{P}}) = C(T)(\delta_p^2 + \bar{\mathbf{P}}^2)^{1/2}/\delta_p$, the right hand side of Eq. (52) vanishes due to the identity

$$n'_f(x)(n_f(y) - 1) + n_f(x)n'_f(y) - n_b(x - y)(n'_f(x) - n'_f(y)) = 0. \tag{54}$$

This is the zero mode of the collision equation, and will lead to an infinite conductivity if excited. However, this mode cannot be excited by the *chiral* electric field as it produces the *same* (instead of *opposite*) deviation in the + and - quasiparticle distributions. This mode will be excited by a *normal* electric field, and is responsible for the infinite DC *charge* conductivity of the system. The modes excited by the chiral electric field obey $\varphi^m(\delta_p, \bar{\mathbf{P}}) = m\varphi(\delta_p, \bar{\mathbf{P}})$ and are orthogonal to the zero mode, yielding a finite *chiral* conductivity (or viscosity).

We have

$$\eta \sim \sigma_{yy} = \frac{J_y}{E_y} = 8(1-d)T \int dp_y p_y^2 \int \frac{d^{d-1}\mathbf{P}}{(2\pi)^d} \frac{p_x^2}{\bar{\mathbf{P}}^2 + p_x^2} n'_f((\bar{\mathbf{P}}^2 + p_x^2)^{1/2}) \varphi(p_x, \bar{\mathbf{P}}), \quad (55)$$

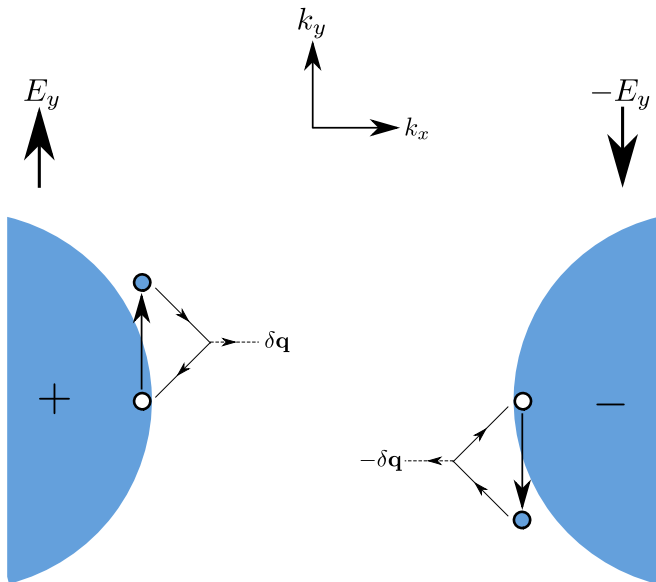


FIG. 3. Elementary excitations due to the chiral electric field that carry a net chiral current at zero total momentum relative to the filled band in a two-patch system. The chiral current can decay via the emission of bosons of opposite momenta on the two patches. Since the individual bosons carry nonzero momentum, the boson distribution responds to the applied chiral electric field and is no longer in equilibrium unlike in a particle-hole symmetric system like those studied in Refs. 56 and 58, where the bosons required to relax the elementary excitations have zero momentum.

where we shifted $p_x \rightarrow p_x - \sqrt{d-1}p_y^2$. Counting powers in Eq. (52), we obtain

$$\varphi(\xi(\mathbf{p}), \bar{\mathbf{P}}) = \beta_d^{1/3} e^{-4/3} \mu^{-2\epsilon/3} T^{-2(d-1)/3-1} \tilde{\varphi}(\xi(\mathbf{p})/T, \bar{\mathbf{P}}/T). \quad (56)$$

Inserting this into Eq. (55) and using the fixed point values of $z^* = 3/(2(d-1))$ and $e^{*4/3} \propto \epsilon^{38}$, we have, to leading order in ϵ ,

$$\eta \sim \frac{1}{\epsilon} T^{-1/z+d-2} \int dp_y p_y^2, \quad (57)$$

which is the expected quantum critical scaling.

If the Boltzmann analysis at this order is performed directly in $d=2$, then the collision equations are solved exactly by using the collisionless momentum-independent

solution for φ , and thus collisions with the boson do not induce a finite DC viscosity. The reason for this is purely kinematic, stemming from the special structure of the patch dispersions in $d=2$ which have Galilean invariance in the y direction and a constant x velocity and was noted earlier in Ref. 59. The quantum critical scaling could possibly be restored by appropriately resumming contributions at higher orders in perturbation theory.

VI. CONCLUSIONS

This paper has exposed the unconventional scaling of the shear viscosity in a theory with a critical Fermi surface. For the Ising-nematic QCP in $d=2$, we computed the optical and DC viscosities in an expansion in $\epsilon = 5/2 - d$ below the upper critical dimension, and showed that the viscosity scales differently than expected from that of a critical point with an effective reduced dimensionality of $(d-1)$ -dimensional excitations transverse to the Fermi surface. As a consequence, the ratio η/s diverges at low temperatures as $T^{-2/z}$ instead of saturating the universal bound like in other strongly-coupled field theories in the literature. We expect that this is a general phenomenon of metallic quantum critical states where hyperscaling is violated due to the presence of a critical Fermi surface, including states described by Fermi surfaces coupled to gauge fields. However, we do expect that metallic critical points associated with singular ‘hot spots’ on the Fermi surface⁵⁸ will have a finite η/s , up to logarithmic factors.

ACKNOWLEDGEMENTS

We thank R. Davison and W. Witczak-Krempa for valuable discussions. This research was supported by the NSF under Grant DMR-1360789 and MURI grant W911NF-14-1-0003 from ARO. Research at Perimeter Institute is supported by the Government of Canada through Industry Canada and by the Province of Ontario through the Ministry of Research and Innovation. AE acknowledges support from the German National Academy of Sciences Leopoldina through grant LPDS 2014-13. SS also acknowledges support from Cenovus Energy at Perimeter Institute. AE and AAP contributed equally to this work.

Appendix A: Optical viscosity: two-loop computations

The two-loop self-energy correction to the stress tensor autocorrelation function is given by

$$\begin{aligned} \langle T_{xy} T_{xy} \rangle_{\text{SE}}(i\omega) &= 2N \int \frac{d^{d+1}k}{(2\pi)^{d+1}} k_y^2 \text{tr} \left(\gamma_x G_0(k+q) \gamma_x G_0(k) \Sigma_1(k) G_0(k) \right) \\ &= 4e^{4/3} u_{\Sigma,0} \epsilon^{-1} \int \frac{d^{d+1}k}{(2\pi)^{d+1}} k_y^2 \left(\frac{\mu}{|\mathbf{K}|} \right)^{2\epsilon/3} \frac{2\delta_k^2 \mathbf{K}^2 + \mathbf{K} \cdot (\mathbf{K} + \mathbf{Q})(\delta_k^2 - \mathbf{K}^2)}{((\mathbf{K} + \mathbf{Q})^2 + \delta_k^2)(\mathbf{K}^2 + \delta_k^2)^2}, \end{aligned} \quad (\text{A1})$$

where we only kept the pole contribution to the self-energy and set $\epsilon = 0$ in the prefactor $u_{\Sigma, \epsilon=0} = (2 \cdot 6^{1/3} \pi)^{-1}$. The self-energy correction can be computed using Feynman parameters. The integral is first rewritten as

$$\langle T_{xy} T_{xy} \rangle_{\text{SE}}(i\omega) = 4(e^2 \mu^\epsilon)^{\frac{2}{3}} u_{\Sigma,0} \epsilon^{-1} \int \frac{d^{d+1}k}{(2\pi)^{d+1}} k_y^2 \int_0^1 dx \frac{1-x}{|\mathbf{K}|^{\frac{2\epsilon}{3}}} \frac{2\delta_k^2 \mathbf{K}^2 + \mathbf{K} \cdot (\mathbf{K} + \mathbf{Q})(\delta_k^2 - \mathbf{K}^2)}{[x(\mathbf{K} + \mathbf{Q})^2 + (1-x)\mathbf{K}^2 + \delta_k^2]^3}. \quad (\text{A2})$$

Eliminating k_y from the fraction by a variable shift of k_x and subsequent integration over k_x yield

$$= \frac{\Gamma(3)}{4} (e^2 \mu^\epsilon)^{\frac{2}{3}} u_{\Sigma,0} \epsilon^{-1} \int \frac{dk_y}{2\pi} k_y^2 \int \frac{d^{d-1}K}{(2\pi)^{d-1}} \int_0^1 dx \frac{1-x}{|\mathbf{K}|^{\frac{2\epsilon}{3}}} \times \left[\frac{3\mathbf{K}^2 + \mathbf{K} \cdot \mathbf{Q}}{[\mathbf{K}^2 + x(2\mathbf{K} \cdot \mathbf{Q} + \mathbf{Q}^2)]^{\frac{3}{2}}} - \frac{3\mathbf{K}^2(\mathbf{K}^2 + \mathbf{K} \cdot \mathbf{Q})}{[\mathbf{K}^2 + x(2\mathbf{K} \cdot \mathbf{Q} + \mathbf{Q}^2)]^{\frac{5}{2}}} \right]. \quad (\text{A3})$$

Again using Feynman parameters to rewrite the products in the integrand, we obtain

$$\begin{aligned} &= \frac{\Gamma(3)}{4\Gamma(\frac{\epsilon}{3})} (e^2 \mu^\epsilon)^{\frac{2}{3}} u_{\Sigma,0} \epsilon^{-1} \int \frac{dk_y}{2\pi} k_y^2 \int \frac{d^{d-1}K}{(2\pi)^{d-1}} \int_0^1 dx \int_0^1 dy \left[\frac{\Gamma(\frac{9+2\epsilon}{6})}{\Gamma(\frac{3}{2})} \frac{(1-x)y^{\frac{\epsilon}{3}-1}(1-y)^{\frac{1}{2}}(3\mathbf{K}^2 + \mathbf{K} \cdot \mathbf{Q})}{[\mathbf{K}^2 + x(1-y)(2\mathbf{K} \cdot \mathbf{Q} + \mathbf{Q}^2)]^{\frac{3}{2} + \frac{\epsilon}{3}}} \right. \\ &\quad \left. - \frac{\Gamma(\frac{15+2\epsilon}{6})}{\Gamma(\frac{5}{2})} \frac{3(1-x)y^{\frac{\epsilon}{3}-1}(1-y)^{\frac{3}{2}}\mathbf{K}^2(\mathbf{K}^2 + \mathbf{K} \cdot \mathbf{Q})}{[\mathbf{K}^2 + x(1-y)(2\mathbf{K} \cdot \mathbf{Q} + \mathbf{Q}^2)]^{\frac{5}{2} + \frac{\epsilon}{3}}} \right]. \end{aligned} \quad (\text{A4})$$

Completing squares in the denominator as

$$\mathbf{K}^2 + x(1-y)(2\mathbf{K} \cdot \mathbf{Q} + \mathbf{Q}^2) = (\mathbf{K} + x(1-y)\mathbf{Q})^2 + x(1-y)(1-x+xy)\mathbf{Q}^2, \quad (\text{A5})$$

shifting $\mathbf{K} \rightarrow \mathbf{K} - x(1-y)\mathbf{Q}$, and neglecting terms that vanish due to symmetries when performing the \mathbf{K} -integration, we obtain

$$\begin{aligned} &= \frac{\Gamma(3)}{4\Gamma(\frac{\epsilon}{3})} (e^2 \mu^\epsilon)^{\frac{2}{3}} u_{\Sigma,0} \epsilon^{-1} \int \frac{dk_y}{2\pi} k_y^2 \int \frac{d^{d-1}K}{(2\pi)^{d-1}} \int_0^1 dx \int_0^1 dy (1-x)y^{\frac{\epsilon}{3}-1} \\ &\quad \times \left\{ \frac{\Gamma(\frac{9+2\epsilon}{6})}{\Gamma(\frac{3}{2})} (1-y)^{\frac{1}{2}} \frac{3\mathbf{K}^2 - x(1-y)(1-3x(1-y))\mathbf{Q}^2}{[\mathbf{K}^2 + x(1-y)(1-y+xy)\mathbf{Q}^2]^{\frac{3}{2} + \frac{\epsilon}{3}}} \right. \\ &\quad \left. - \frac{\Gamma(\frac{15+2\epsilon}{6})}{\Gamma(\frac{5}{2})} \frac{3(1-y)^{\frac{3}{2}}}{[\mathbf{K}^2 + x(1-y)(1-x+xy)\mathbf{Q}^2]^{\frac{5}{2} + \frac{\epsilon}{3}}} \left[\mathbf{K}^4 - x(1-y)(1-2x(1-y))\mathbf{K}^2\mathbf{Q}^2 \right. \right. \\ &\quad \left. \left. - 2x(1-y)(1-2x(1-y))(\mathbf{K} \cdot \mathbf{Q})^2 - x^3(1-y)^3(1-x(1-y))\mathbf{Q}^4 \right] \right\} \end{aligned} \quad (\text{A6})$$

The remaining integrals can easily be computed using *Mathematica*. First integrating over \mathbf{K} and subsequently over x and y , the pole contribution to the two-loop self-energy correction reads

$$\langle T_{xy} T_{xy} \rangle_{\text{SE}}(i\omega) = e^{4/3} \epsilon^{-1} \int \frac{dk_y}{2\pi} k_y^2 |\omega|^{\frac{1}{2}-\epsilon} \left(\frac{\mu}{|\omega|} \right)^{2\epsilon/3} a_{\Sigma,0}, \quad (\text{A7})$$

where $a_{\Sigma,0} = u_{1\text{Loop},0} u_{\Sigma,0}$, after setting ϵ to zero in the numerical prefactors.

Appendix B: Relating conductivities and viscosities using Ward identities

The result in the main text, that the optical viscosity and optical conductivity scale in the same way, is not consistent with hyperscaling with an effectively reduced dimension. In order to substantiate this result, in the following we establish relations between the two transport quantities based on Ward identities.

The action for the patch theory of the Ising-nematic QCP in $d = 2$, Eq. (11), is invariant under an emergent rotational symmetry³⁷,

$$\Phi(q_0, q_x, q_y) \rightarrow \Phi'(q_0, q_x, q_y) = \Phi(q_0, q_x - \Theta q_y, q_y) \quad (\text{B1})$$

$$\tilde{\psi}_{sj}(k_0, k_x, k_y) \rightarrow \tilde{\psi}'_{sj}(k_0, k_x, k_y) = \tilde{\psi}_{sj}\left(k_0, k_x - \Theta k_y - s\frac{\Theta^2}{4}, k_y + s\frac{\Theta}{2}\right). \quad (\text{B2})$$

We will show that this symmetry restricts the scaling behavior of transport properties as a function of frequency. Starting from this transformation law, we derive a Ward identity for the generating functional of connected correlation functions⁶⁰,

$$\mathcal{G}[\eta^\dagger, \eta, \phi] = \ln Z[\eta^\dagger, \eta, \phi] \quad (\text{B3})$$

$$Z[\eta^\dagger, \eta, \phi] = \int D(\tilde{\psi}^\dagger, \tilde{\psi}) D(\Phi) e^{-S[\tilde{\psi}^\dagger, \tilde{\psi}, \Phi] - \int_k \sum_{s,j} (\tilde{\psi}_{sj}^\dagger(k) \eta_{sj}(k) + \eta_{sj}^\dagger(k) \tilde{\psi}_{sj}(k)) - \int_q \Phi(-q) \phi(q)}, \quad (\text{B4})$$

where $\eta^{(\dagger)}$ and ϕ are Grassmann and real source fields, respectively. Invariance under the above rotational symmetry implies

$$\mathcal{G}[\eta'^\dagger, \eta', \phi'] = \mathcal{G}[\eta^\dagger, \eta, \phi], \quad (\text{B5})$$

where the source fields transform as the physical fields. Differentiation with respect to Θ yields

$$\frac{d}{d\Theta} \mathcal{G}[\eta'^\dagger, \eta', \phi'] = 0, \quad (\text{B6})$$

which leads to the functional Ward identity

$$\begin{aligned} \int \frac{d^3 k}{(2\pi)^3} \sum_{s,j} \left\{ \left[(k_y \partial_{k_x} \eta_{sj}^\dagger(k) - \frac{s}{2} \partial_{k_y} \eta_{sj}^\dagger(k)) \frac{\delta Z[\eta^\dagger, \eta, \phi]}{\delta \eta_{sj}^\dagger(k)} + (k_y \partial_{k_x} \eta_{sj}(k) - \frac{s}{2} \partial_{k_y} \eta_{sj}(k)) \frac{\delta Z[\eta^\dagger, \eta, \phi]}{\delta \eta_{sj}(k)} \right] \right. \\ \left. - \int_q q_y \partial_{q_x} \phi(q) \frac{\delta Z[\eta^\dagger, \eta, \phi]}{\delta \phi(q)} \right\} = 0. \end{aligned} \quad (\text{B7})$$

In the following we are only interested in Ward identities for fermionic correlation functions and thus set $\phi = 0$ from the outset.

As an example how this functional Ward identity restricts correlation functions, we derive the Ward identity that follows from rotational symmetry for the fermionic Green's function. After computing suitable functional derivatives, we obtain

$$(p_y \partial_{p_x} - \frac{s}{2} \partial_{p_y}) \frac{\delta^2 Z[\eta^\dagger, \eta, 0]}{\partial \eta_{sj}(p) \partial \eta_{sj}^\dagger(p)} \Big|_{\eta=\eta^\dagger=0} = -(p_y \partial_{p_x} - \frac{s}{2} \partial_{p_y}) G_s(p) = 0, \quad (\text{B8})$$

where $G_s(p)$ is the full fermionic Green's function. This is a partial differential equation for the momentum dependence of the latter. It can easily be verified that the Ward identity is fulfilled for $G_s(p) = G_s(p_0, sp_x + p_y^2)$, as expected.

For $q = q_0 \mathbf{e}_0 \neq 0$, the current-current correlation functions for the chiral current can be written as

$$\begin{aligned} \langle J_x(q) J_x(-q) \rangle &= \int \frac{d^3 k}{(2\pi)^3} \int \frac{d^3 k'}{(2\pi)^3} \sum_{j,s,j',s'} \langle \tilde{\psi}_{js}^\dagger(k+q) \tilde{\psi}_{js}(k) \tilde{\psi}_{j's'}^\dagger(k'-q) \tilde{\psi}_{j's'}(k') \rangle \\ &= Z^{-1} \int \frac{d^3 k}{(2\pi)^3} \int \frac{d^3 k'}{(2\pi)^3} \sum_{j,s,j',s'} \frac{\delta^4 Z[\eta^\dagger, \eta, 0]}{\delta \eta_{js}(k+q) \delta \eta_{js}^\dagger(k) \delta \eta_{j's'}(k'-q) \delta \eta_{j's'}^\dagger(k')} \Big|_{\eta=\eta^\dagger=0} \end{aligned} \quad (\text{B9})$$

$$\begin{aligned} \langle J_y(q) J_y(-q) \rangle &= 4 \langle T_{xy}(q) T_{xy}(-q) \rangle \\ &= 4 \int \frac{d^3 k}{(2\pi)^3} \int \frac{d^3 k'}{(2\pi)^3} \sum_{j,s,j',s'} ss' k_y k'_y \langle \tilde{\psi}_{js}^\dagger(k+q) \tilde{\psi}_{js}(k) \tilde{\psi}_{j's'}^\dagger(k'-q) \tilde{\psi}_{j's'}(k') \rangle \\ &= 4Z^{-1} \int \frac{d^3 k}{(2\pi)^3} \int \frac{d^3 k'}{(2\pi)^3} \sum_{j,s,j',s'} ss' k_y k'_y \frac{\delta^4 Z[\eta^\dagger, \eta, 0]}{\delta \eta_{js}(k+q) \delta \eta_{js}^\dagger(k) \delta \eta_{j's'}(k'-q) \delta \eta_{j's'}^\dagger(k')} \Big|_{\eta=\eta^\dagger=0}. \end{aligned} \quad (\text{B10})$$

Applying functional derivatives to the functional Ward identity Eq. (B7), we obtain a Ward identity for two-particle Green's functions,

$$\left[(k_y \partial_{k_x} - \frac{s}{2} \partial_{k_y}) + (k'_y \partial_{k'_x} - \frac{s'}{2} \partial_{k'_y}) \right] \frac{\delta^4 Z[\eta^\dagger, \eta, 0]}{\delta \eta_{js}(k+q) \delta \eta_{js}^\dagger(k) \delta \eta_{j's'}(k'-q) \delta \eta_{j's'}^\dagger(k')} \Big|_{\eta=\eta^\dagger=0} = 0. \quad (\text{B11})$$

Using the method of characteristics, we can show that this Ward identity restricts the dependence of two-particle Green's function on spatial momenta as

$$\frac{\delta^4 Z[\eta^\dagger, \eta, 0]}{\delta \eta_{js}(k+q) \delta \eta_{js}^\dagger(k) \delta \eta_{j's'}(k'-q) \delta \eta_{j's'}^\dagger(k')} \Big|_{\eta=\eta^\dagger=0} = F_{js;j's'}(k_0, k'_0, q_0; sk_x + k_y^2, s'k'_x + k_y'^2, s'k_y - sk'_y), \quad (\text{B12})$$

analogously to the Ward identity for the one-particle Green's function.

Inserting this result in Eqs. (B9) and (B10), shifting and renaming integration variables, we obtain for the J_x correlator

$$\begin{aligned} \langle J_x(q_0) J_x(-q_0) \rangle &= Z^{-1} \int \frac{d^3 k}{(2\pi)^3} \int \frac{d^3 k'}{(2\pi)^3} \sum_{j,s,j',s'} F_{js;j's'}(k_0, k'_0, q_0; sk_x + k_y^2, s'k'_x + k_y'^2, s'k_y - sk'_y) \\ &= Z^{-1} \int \frac{d^3 k}{(2\pi)^3} \int \frac{d^3 k'}{(2\pi)^3} \sum_{j,s,j',s'} F_{js;j's'}(k_0, k'_0, q_0; k_x, k'_x, k_y). \end{aligned} \quad (\text{B13})$$

Note that k'_y does not appear in the integrand. For the J_y correlator we obtain

$$\begin{aligned} \langle J_y(q_0) J_y(-q_0) \rangle &= 4Z^{-1} \int \frac{d^3 k}{(2\pi)^3} \int \frac{d^3 k'}{(2\pi)^3} \sum_{j,s,j',s'} ss' k_y k'_y F_{js;j's'}(k_0, k'_0, q_0; sk_x + k_y^2, s'k'_x + k_y'^2, s'k_y - sk'_y) \\ &= 4Z^{-1} \int \frac{d^3 k}{(2\pi)^3} \int \frac{d^3 k'}{(2\pi)^3} \sum_{j,s,j',s'} k_y k'_y F_{js;j's'}(k_0, k'_0, q_0; k_x, k'_x, k_y - k'_y) \\ &= 2Z^{-1} \int \frac{d^3 k}{(2\pi)^3} \int \frac{d^3 k'}{(2\pi)^3} \sum_{j,s,j',s'} (k_y + k'_y) k'_y F_{js;j's'}(k_0, k'_0, q_0; k_x, k'_x, k_y) \\ &\quad + 2Z^{-1} \int \frac{d^3 k}{(2\pi)^3} \int \frac{d^3 k'}{(2\pi)^3} \sum_{j,s,j',s'} k_y (k_y + k'_y) F_{js;j's'}(k_0, k'_0, q_0; k_x, k'_x, -k'_y) \end{aligned} \quad (\text{B14})$$

where in the last step we shifted $k_y \rightarrow k_y + k'_y$ and $k'_y \rightarrow k'_y + k_y$ in the first and second term, respectively. Replacing $k'_y \rightarrow -k'_y$ and subsequently renaming $k_y \leftrightarrow k'_y$ in the second term, the contributions $\sim k_y k'_y$ cancel and we hence obtain

$$= 4Z^{-1} \int \frac{d^3 k}{(2\pi)^3} \int \frac{d^3 k'}{(2\pi)^3} \sum_{j,s,j',s'} k_y'^2 F_{js;j's'}(k_0, k'_0, q_0; k_x, k'_x, k_y). \quad (\text{B15})$$

Using the Ward identity for the emergent rotational symmetry of the patch theory, we have thus established that

$$\langle J_x(q_0) J_x(-q_0) \rangle = \frac{\int \frac{dk_y}{(2\pi)}}{4 \int \frac{dk_y}{(2\pi)} k_y^2} \langle J_y(q_0) J_y(-q_0) \rangle = \frac{\int \frac{dk_y}{(2\pi)}}{\int \frac{dk_y}{(2\pi)} k_y^2} \langle T_{xy}(q_0) T_{xy}(-q_0) \rangle. \quad (\text{B16})$$

As the Ward identity imposes restrictions only on the momentum dependence of the two-particle Green's function, this result is also valid in $d = 5/2 - \epsilon$. The above result implies that the optical viscosity and the optical (chiral) conductivity have the same frequency dependence,

$$\sigma(\omega) \sim \eta(\omega). \quad (\text{B17})$$

Using the results from Ref. 54, we obtain

$$\sigma(\omega) \sim \eta(\omega) \sim \omega^{-1/2-\epsilon/3} \stackrel{\epsilon=1/2}{=} \omega^{-2/3}, \quad (\text{B18})$$

in agreement with the field theoretic result in Eq. (33).

Appendix C: Contributions from the full Fermi surface

The result Eq. (B18) for the scaling of the optical viscosity was derived in the patch theory. The question arises whether the scaling could be different for the full Fermi surface, for example due to some preferred direction. In this section we show that this is not the case, using $d = 2$ for simplicity.

We first analyze how the T_{xy} correlator transforms under the emergent rotation symmetry of the patch theory³⁷. In $d = 2$, T_{xy} is given by

$$T_{xy}(q) = \sum_{j,s,s'} \int_{\mathbf{k}} \left(k_y + \frac{q_y}{2}\right) \tilde{\psi}_{sj}^\dagger(\mathbf{k} + \mathbf{q}) \sigma_{z,ss'} \tilde{\psi}_{s'j}(\mathbf{k}). \quad (\text{C1})$$

We obtain

$$\langle T_{xy} T_{xy} \rangle_{\text{1Loop}}(q) \stackrel{q=\omega e_0}{=} -N \int_{\mathbf{k}} k_y^2 \text{tr}(G_0(k_0 + \omega, \mathbf{k}) G_0(k_0, \mathbf{k})) \quad (\text{C2})$$

for the correlation function, where we exploited in the last step that G_0 and σ_z commute. Rotation of the Fermi momentum, with respect to which the patch theory is defined, by a small angle θ yields

$$\langle T_{xy} T_{xy} \rangle_{\text{1Loop}}(q) = -N \int_{\mathbf{k}} \sum_s \left(k_y + s \frac{\theta}{2}\right)^2 G_{0,s}(k_0 + \omega, \mathbf{k}) G_{0,s}(k_0, \mathbf{k}), \quad (\text{C3})$$

where

$$k_x \rightarrow k_x - \theta k_y - s \frac{\theta^2}{4}, \quad k_y \rightarrow k_y + s \frac{\theta}{2}. \quad (\text{C4})$$

The Green's functions are independent of θ due to the emergent rotation symmetry. We can therefore eliminate k_y from the Green's functions by shifting $k_x \rightarrow k_x - s k_y^2$. Then θ only appears in the integrand of the k_y integral, which is just a multiplicative prefactor, and can be eliminated by shifting $k_y \rightarrow k_y - s \frac{\theta}{2}$. Nearby patches thus contribute equally to the T_{xy} correlator.

This result can be complemented by an analysis of the stress tensor correlation function for a continuum model. For an isotropic system we can start from the Lagrangian

$$\mathcal{L}(x) = \psi^\dagger(x) \partial_\tau \psi(x) + \nabla \psi^\dagger(x) \cdot \nabla \psi(x) - \mu \psi^\dagger(x) \psi(x), \quad (\text{C5})$$

where we omitted the interaction and the bosonic contribution. The xy -component of the stress tensor reads

$$T_{xy}(q) = \int_{\mathbf{k}} ((k_x + q_x) k_y + (k_y + q_y) k_x) \psi^\dagger(\mathbf{k} + \mathbf{q}) \psi(\mathbf{k}). \quad (\text{C6})$$

At one-loop level, the T_{xy} autocorrelation function for $\mathbf{q} = 0$ is then given by

$$\langle T_{xy} T_{xy} \rangle_{\text{1Loop}}(i\omega) = -4 \int_{\mathbf{k}} k_x^2 k_y^2 G_0(k + \mathbf{q}) G_0(k) \quad (\text{C7})$$

where $q = \omega e_0$.

We can subdivide the vicinity of the Fermi surface into (finite) patches, which are labeled by ϕ , and obtain

$$\langle T_{xy} T_{xy} \rangle_{\text{1Loop}}(i\omega) = -4 \sum_{\text{Patches}} \int_{\mathbf{k}'} (k'_x \cos \phi - k'_y \sin \phi)^2 (k'_x \sin \phi + k'_y \cos \phi)^2 \text{tr}(G_0(k'_0 + \omega, \mathbf{k}') G_0(k'_0, \mathbf{k}')), \quad (\text{C8})$$

where the integral over \mathbf{k}' is over a specific patch. The sum over patches (or ϕ -integration) sums up the contributions from individual patches. The Green's functions do not depend on ϕ because they are the same in each local patch coordinate system (Fig. 4) and are just given by the patch theory action in the supplement. Shifting $k'_x \rightarrow k_F + k'_x$ in order to make the Fermi momentum explicit, we obtain

$$\begin{aligned} (k'_x \cos \phi - k'_y \sin \phi)^2 (k'_x \sin \phi + k'_y \cos \phi)^2 &\rightarrow \frac{1}{4} \left(2k_F k'_y \cos(2\phi) + k_F^2 \sin(2\phi) - k_y'^2 \sin(2\phi) \right)^2 \\ &+ \frac{1}{4} k_x'^2 \left(6k_F k'_y \sin(4\phi) + 6k_F^2 \sin^2(2\phi) + k_y'^2 (3 \cos(4\phi) + 1) \right) \\ &+ \frac{1}{2} k_x' \left(3k_F^2 k'_y \sin(4\phi) + k_F k_y'^2 (3 \cos(4\phi) + 1) + 2k_F^3 \sin^2(2\phi) - k_y'^3 \sin(4\phi) \right) \\ &+ k_x'^3 \sin(2\phi) (k_F \sin(2\phi) + k'_y \cos(2\phi)) + k_x'^4 \sin^2 \phi \cos^2 \phi. \end{aligned} \quad (\text{C9})$$

The terms in the first line of the right hand side do not depend on k'_x and yield the scaling that we determined from the patch theory as k'_y and k_F do not scale. The terms on the other lines contain additional powers of $k'_x \sim \omega^{1/z}$ and are hence subleading. The above argument takes care of the 1-loop and self-energy corrections. In the vertex corrections,

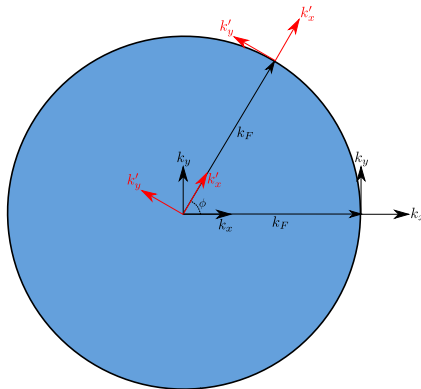


FIG. 4. Transformation of coordinates used to determine the contribution of different patches to the $T_{xy} - T_{xy}$ correlator.

the additional powers of k'_x and k'_y do not influence the absence of poles in ϵ^{-1} . Hence all patches contribute the same scaling at leading order in ω .

The expressions in Eqs. (C2) and (C7) are directly related only for the patches in the k_x or the k_y direction. In the former case, evaluating the factor $k_x^2 k_y^2$ in the integrand close to the Fermi surface yields $(k_F + k'_x)^2 k_y'^2 \approx k_F^2 k_y'^2$. After rescaling of momentum variables, this yields the factor of k_y^2 that appears in the stress tensor correlation function of the patch theory in Eq. (C2). For other directions additional terms appear, which are not present in the patch theory, for example terms in Eq. (C9) which are proportional to k_F^4 . As k_F and k_y do not scale, such terms are equally relevant to the terms that appear in the patch theory and thus do not change the scaling behavior. The argument employing the emergent rotational symmetry does not generate such terms, but nevertheless leads to the correct scaling behavior.

-
- ¹ D. A. Bandurin, I. Torre, R. K. Kumar, M. Ben Shalom, A. Tomadin, A. Principi, G. H. Auton, E. Khestanova, K. S. Novoselov, I. V. Grigorieva, L. A. Ponomarenko, A. K. Geim, and M. Polini, “Negative local resistance caused by viscous electron backflow in graphene,” *Science* **351**, 1055 (2016), [arXiv:1509.04165 \[cond-mat.str-el\]](#).
 - ² J. Crossno, J. K. Shi, K. Wang, X. Liu, A. Harzheim, A. Lucas, S. Sachdev, P. Kim, T. Taniguchi, K. Watanabe, T. A. Ohki, and K. C. Fong, “Observation of the Dirac fluid and the breakdown of the Wiedemann-Franz law in graphene,” *Science* **351**, 1058 (2016), [arXiv:1509.04713 \[cond-mat.mes-hall\]](#).
 - ³ P. J. W. Moll, P. Kushwaha, N. Nandi, B. Schmidt, and A. P. Mackenzie, “Evidence for hydrodynamic electron flow in PdCoO₂,” *Science* **351**, 1061 (2016), [arXiv:1509.05691 \[cond-mat.str-el\]](#).
 - ⁴ R. N. Gurzhi, “Hydrodynamic effects in solids at low temperatures,” *Sov. Phys. Usp.* **11**, 255 (1968).
 - ⁵ M. J. M. de Jong and L. W. Molenkamp, “Hydrodynamic electron flow in high-mobility wires,” *Phys. Rev. B* **51**, 13389 (1995), [cond-mat/9411067](#).
 - ⁶ A. V. Andreev, S. A. Kivelson, and B. Spivak, “Hydrodynamic Description of Transport in Strongly Correlated Electron Systems,” *Phys. Rev. Lett.* **106**, 256804 (2011), [arXiv:1011.3068 \[cond-mat.mes-hall\]](#).
 - ⁷ K. Damle and S. Sachdev, “Nonzero-temperature transport near quantum critical points,” *Phys. Rev. B* **56**, 8714 (1997), [cond-mat/9705206](#).
 - ⁸ S. A. Hartnoll, P. K. Kovtun, M. Müller, and S. Sachdev, “Theory of the Nernst effect near quantum phase transitions in condensed matter and in dyonic black holes,” *Phys. Rev. B* **76**, 144502 (2007), [arXiv:0706.3215 \[cond-mat.str-el\]](#).
 - ⁹ S. A. Hartnoll, R. Mahajan, M. Punk, and S. Sachdev, “Transport near the Ising-nematic quantum critical point of metals in two dimensions,” *Phys. Rev. B* **89**, 155130 (2014), [arXiv:1401.7012 \[cond-mat.str-el\]](#).
 - ¹⁰ A. A. Patel and S. Sachdev, “DC resistivity at the onset of spin density wave order in two-dimensional metals,” *Phys. Rev. B* **90**, 165146 (2014), [arXiv:1408.6549 \[cond-mat.str-el\]](#).
 - ¹¹ A. Lucas and S. Sachdev, “Memory matrix theory of magnetotransport in strange metals,” *Phys. Rev. B* **91**, 195122 (2015), [arXiv:1502.04704 \[cond-mat.str-el\]](#).
 - ¹² M. Müller and S. Sachdev, “Collective cyclotron motion of the relativistic plasma in graphene,” *Phys. Rev. B* **78**, 115419 (2008), [arXiv:0801.2970 \[cond-mat.str-el\]](#).
 - ¹³ L. Fritz, J. Schmalian, M. Müller, and S. Sachdev, “Quan-

- tum critical transport in clean graphene,” *Phys. Rev. B* **78**, 085416 (2008), [arXiv:0802.4289](#).
- 14 M. Müller, L. Fritz, and S. Sachdev, “Quantum-critical relativistic magnetotransport in graphene,” *Phys. Rev. B* **78**, 115406 (2008), [arXiv:0805.1413 \[cond-mat.str-el\]](#).
 - 15 M. S. Foster and I. L. Aleiner, “Slow imbalance relaxation and thermoelectric transport in graphene,” *Phys. Rev. B* **79**, 085415 (2009), [arXiv:0810.4342 \[cond-mat.mes-hall\]](#).
 - 16 M. Müller, J. Schmalian, and L. Fritz, “Graphene: A Nearly Perfect Fluid,” *Phys. Rev. Lett.* **103**, 025301 (2009), [arXiv:0903.4178 \[cond-mat.mes-hall\]](#).
 - 17 M. Mendoza, H. J. Herrmann, and S. Succi, “Preturbulent Regimes in Graphene Flow,” *Phys. Rev. Lett.* **106**, 156601 (2011), [arXiv:1201.6590 \[cond-mat.mes-hall\]](#).
 - 18 A. Tomadin, G. Vignale, and M. Polini, “Corbino Disk Viscometer for 2D Quantum Electron Liquids,” *Phys. Rev. Lett.* **113**, 235901 (2014), [arXiv:1401.0938 \[cond-mat.mes-hall\]](#).
 - 19 A. Principi and G. Vignale, “Violation of the Wiedemann-Franz Law in Hydrodynamic Electron Liquids,” *Phys. Rev. Lett.* **115**, 056603 (2015), [arXiv:1406.2940 \[cond-mat.mes-hall\]](#).
 - 20 I. Torre, A. Tomadin, A. K. Geim, and M. Polini, “Nonlocal transport and the hydrodynamic shear viscosity in graphene,” *Phys. Rev. B* **92**, 165433 (2015), [arXiv:1508.00363 \[cond-mat.mes-hall\]](#).
 - 21 L. Levitov and G. Falkovich, “Electron viscosity, current vortices and negative nonlocal resistance in graphene,” *Nat Phys* **12**, 672 (2016), [arXiv:1508.00836 \[cond-mat.mes-hall\]](#).
 - 22 A. Lucas, J. Crossno, K. C. Fong, P. Kim, and S. Sachdev, “Transport in inhomogeneous quantum critical fluids and in the Dirac fluid in graphene,” *Phys. Rev. B* **93**, 075426 (2016), [arXiv:1510.01738 \[cond-mat.str-el\]](#).
 - 23 G. Falkovich and L. Levitov, “Linking Spatial Distributions of Potential and Current in Viscous Electronics,” *ArXiv e-prints* (2016), [arXiv:1607.00986 \[cond-mat.mes-hall\]](#).
 - 24 G. Policastro, D. T. Son, and A. O. Starinets, “Shear Viscosity of Strongly Coupled $N = 4$ Supersymmetric Yang-Mills Plasma,” *Phys. Rev. Lett.* **87**, 081601 (2001), [hep-th/0104066](#).
 - 25 P. K. Kovtun, D. T. Son, and A. O. Starinets, “Viscosity in Strongly Interacting Quantum Field Theories from Black Hole Physics,” *Phys. Rev. Lett.* **94**, 111601 (2005), [hep-th/0405231](#).
 - 26 F. Karsch, D. Kharzeev, and K. Tuchin, “Universal properties of bulk viscosity near the QCD phase transition,” *Phys. Lett. B* **663**, 217 (2008), [arXiv:0711.0914 \[hep-ph\]](#).
 - 27 U. Heinz, C. Shen, and H. Song, “The viscosity of quark-gluon plasma at RHIC and the LHC,” in *American Institute of Physics Conference Series*, American Institute of Physics Conference Series, Vol. 1441, edited by S. G. Steadman, G. S. F. Stephans, and F. E. Taylor (2012) pp. 766–770, [arXiv:1108.5323 \[nucl-th\]](#).
 - 28 C. Cao, E. Elliott, J. Joseph, H. Wu, J. Petricka, T. Schäfer, and J. E. Thomas, “Universal Quantum Viscosity in a Unitary Fermi Gas,” *Science* **331**, 58 (2011), [arXiv:1007.2625 \[cond-mat.quant-gas\]](#).
 - 29 E. Taylor and M. Randeria, “Viscosity of strongly interacting quantum fluids: Spectral functions and sum rules,” *Phys. Rev. A* **81**, 053610 (2010), [arXiv:1002.0869 \[cond-mat.quant-gas\]](#).
 - 30 T. Enss, R. Haussmann, and W. Zwerger, “Viscosity and scale invariance in the unitary Fermi gas,” *Annals of Physics* **326**, 770 (2011), [arXiv:1008.0007 \[cond-mat.quant-gas\]](#).
 - 31 A. Kryjevski, “Shear viscosity of the normal phase of a unitary Fermi gas from the ϵ expansion,” *Phys. Rev. A* **89**, 023621 (2014), [arXiv:1206.0059 \[cond-mat.quant-gas\]](#).
 - 32 M. Bluhm and T. Schäfer, “Model-Independent Determination of the Shear Viscosity of a Trapped Unitary Fermi gas: Application to High-Temperature Data,” *Phys. Rev. Lett.* **116**, 115301 (2016), [arXiv:1512.00862 \[cond-mat.quant-gas\]](#).
 - 33 J. D. Rameau, T. J. Reber, H.-B. Yang, S. Akhanejee, G. D. Gu, P. D. Johnson, and S. Campbell, “Nearly perfect fluidity in a high-temperature superconductor,” *Phys. Rev. B* **90**, 134509 (2014), [arXiv:1409.5820 \[cond-mat.str-el\]](#).
 - 34 C. J. Halboth and W. Metzner, “ d -Wave Superconductivity and Pomeranchuk Instability in the Two-Dimensional Hubbard Model,” *Phys. Rev. Lett.* **85**, 5162 (2000), [cond-mat/0003349](#).
 - 35 V. Oganesyan, S. A. Kivelson, and E. Fradkin, “Quantum theory of a nematic Fermi fluid,” *Phys. Rev. B* **64**, 195109 (2001), [cond-mat/0102093](#).
 - 36 W. Metzner, D. Rohe, and S. Andergassen, “Soft Fermi Surfaces and Breakdown of Fermi-Liquid Behavior,” *Phys. Rev. Lett.* **91**, 066402 (2003), [cond-mat/0303154](#).
 - 37 M. A. Metlitski and S. Sachdev, “Quantum phase transitions of metals in two spatial dimensions. I. Ising-nematic order,” *Phys. Rev. B* **82**, 075127 (2010), [arXiv:1001.1153 \[cond-mat.str-el\]](#).
 - 38 D. Dalidovich and S.-S. Lee, “Perturbative non-Fermi liquids from dimensional regularization,” *Phys. Rev. B* **88**, 245106 (2013), [arXiv:1307.3170 \[cond-mat.str-el\]](#).
 - 39 P. Kovtun, “Lectures on hydrodynamic fluctuations in relativistic theories,” *J. Phys. A Math. Gen.* **45**, 473001 (2012), [arXiv:1205.5040 \[hep-th\]](#).
 - 40 N. Iqbal and H. Liu, “Universality of the hydrodynamic limit in AdS/CFT and the membrane paradigm,” *Phys. Rev. D* **79**, 025023 (2009), [arXiv:0809.3808 \[hep-th\]](#).
 - 41 D. Roychowdhury, “Hydrodynamics from scalar black branes,” *JHEP* **4**, 162 (2015), [arXiv:1502.04345 \[hep-th\]](#).
 - 42 E. Kiritsis and Y. Matsuo, “Charge-hyperscaling violating Lifshitz hydrodynamics from black-holes,” *JHEP* **12**, 76 (2015), [arXiv:1508.02494 \[hep-th\]](#).
 - 43 X.-M. Kuang and J.-P. Wu, “Transport coefficients from hyperscaling violating black brane: shear viscosity and conductivity,” *ArXiv e-prints* (2015), [arXiv:1511.03008 \[hep-th\]](#).
 - 44 K. S. Kolekar, D. Mukherjee, and K. Narayan, “Hyperscaling violation and the shear diffusion constant,” *Phys. Lett. B* **760**, 86 (2016), [arXiv:1604.05092 \[hep-th\]](#).
 - 45 H. Liu, J. McGreevy, and D. Vegh, “Non-Fermi liquids from holography,” *Phys. Rev. D* **83**, 065029 (2011), [arXiv:0903.2477 \[hep-th\]](#).
 - 46 M. Čubrović, J. Zaanen, and K. Schalm, “String Theory, Quantum Phase Transitions, and the Emergent Fermi Liquid,” *Science* **325**, 439 (2009), [arXiv:0904.1993 \[hep-th\]](#).
 - 47 C. Charmousis, B. Gouteraux, B. S. Kim, E. Kiritsis, and R. Meyer, “Effective Holographic Theories for low-temperature condensed matter systems,” *JHEP* **11**, 151 (2010), [arXiv:1005.4690 \[hep-th\]](#).
 - 48 K. Goldstein, S. Kachru, S. Prakash, and S. P. Trivedi, “Holography of Charged Dilaton Black Holes,” *JHEP* **08**, 078 (2010), [arXiv:0911.3586 \[hep-th\]](#).
 - 49 N. Ogawa, T. Takayanagi, and T. Ugajin, “Holographic

- Fermi Surfaces and Entanglement Entropy,” *JHEP* **01**, 125 (2012), [arXiv:1111.1023 \[hep-th\]](#).
- ⁵⁰ L. Huijse, S. Sachdev, and B. Swingle, “Hidden Fermi surfaces in compressible states of gauge-gravity duality,” *Phys. Rev. B* **85**, 035121 (2012), [arXiv:1112.0573 \[cond-mat.str-el\]](#).
- ⁵¹ J. Polchinski and E. Silverstein, “Large-density field theory, viscosity, and ‘ $2k_F$ ’ singularities from string duals,” *Class. Quant. Grav.* **29**, 194008 (2012), [arXiv:1203.1015 \[hep-th\]](#).
- ⁵² T. Faulkner and N. Iqbal, “Friedel oscillations and horizon charge in 1D holographic liquids,” *JHEP* **07**, 060 (2013), [arXiv:1207.4208 \[hep-th\]](#).
- ⁵³ S. Sachdev, “Compressible quantum phases from conformal field theories in 2+1 dimensions,” *Phys. Rev. D* **86**, 126003 (2012), [arXiv:1209.1637 \[hep-th\]](#).
- ⁵⁴ A. Eberlein, I. Mandal, and S. Sachdev, “Hyperscaling violation at the Ising-nematic quantum critical point in two-dimensional metals,” *Phys. Rev. B* **94**, 045133 (2016), [arXiv:1605.00657 \[cond-mat.str-el\]](#).
- ⁵⁵ M. D. Schwartz, *Quantum field theory and the standard model* (Cambridge University Press, 2014).
- ⁵⁶ L. Fritz, “Quantum critical transport at a semimetal-to-insulator transition on the honeycomb lattice,” *Phys. Rev. B* **83**, 035125 (2011), [arXiv:1012.0263 \[cond-mat.str-el\]](#).
- ⁵⁷ A. Kamenev, *Field Theory of Non-Equilibrium Systems* (Cambridge University Press, Cambridge, UK, 2011).
- ⁵⁸ A. A. Patel, P. Strack, and S. Sachdev, “Hyperscaling at the spin density wave quantum critical point in two-dimensional metals,” *Phys. Rev. B* **92**, 165105 (2015), [arXiv:1507.05962 \[cond-mat.str-el\]](#).
- ⁵⁹ D. L. Maslov, V. I. Yudson, and A. V. Chubukov, “Resistivity of a Non-Galilean-Invariant Fermi Liquid near Pomeranchuk Quantum Criticality,” *Phys. Rev. Lett.* **106**, 106403 (2011), [arXiv:1012.0069 \[cond-mat.str-el\]](#).
- ⁶⁰ J. W. Negele and H. Orland, *Quantum Many-Particle Systems*, edited by D. Pines, Advanced Book Classics (Westview Press, Reading, Massachusetts, 1998).